

Angular momentum transport by internal gravity waves

II. Pop II stars from the Li plateau to the horizontal branch

S. Talon¹ and C. Charbonnel^{2,3}

¹ Département de Physique, Université de Montréal, Montréal PQ H3C 3J7, Canada
e-mail: Suzanne.Talon@astro.umontreal.ca

² Laboratoire d'Astrophysique de l'Observatoire Midi-Pyrénées, CNRS UMR 5572, 14, Av. E. Belin, 31400 Toulouse, France

³ Observatoire de Genève, 51, Ch. des Maillettes, 1290 Sauverny, Switzerland

Received 17 September 2003 / Accepted 15 January 2004

Abstract. This paper is the second in a series where we examine the generation and filtering of internal gravity waves in stars and the consequences of wave-induced transport of angular momentum at various stages of stellar evolution. Here we concentrate on Pop II dwarf stars and we focus in particular on the differential properties of internal gravity waves as a function of the stellar mass. We show that, for the range of masses corresponding to the lithium plateau, gravity waves are fully efficient and should thus lead to a quasi-solid rotation state, similar to that of the Sun. In the slightly more massive progenitors of currently observed horizontal branch star however, internal wave generation is not efficient on the main sequence, and large internal differential rotation can thus be maintained. This leads to a natural explanation of the large rotational velocities measured on the horizontal branch in some globular clusters.

Key words. hydrodynamics – stars: interiors – stars: rotation – stars: abundances – stars: Population II – waves

1. The Li plateau

The study of lithium abundances in metal-poor halo stars has crucial implications for stellar structure, galactic evolution, and cosmology. Since its discovery by Spite & Spite (1982), the so-called lithium plateau¹ has been the subject of considerable observational and theoretical effort. Of main importance is the question of the “uniformity” of lithium abundances in Population II stars, and there has been a spirited debate about the existence and magnitude in halo star data of dispersion and trends with metallicity and effective temperature. (We refer to Primas & Charbonnel 2004 for a detailed review of the literature.)

On the one hand, the slope with [Fe/H] mainly constrains the contribution of galactic chemical evolution to the observed lithium abundance and in particular the rate of cosmic ray spallations in the early Galaxy while the trend with T_{eff} principally constrains the mass dependence of the internal physics of stars. On the other hand the existence or absence of a detectable range in abundance at fixed T_{eff} and [Fe/H] should be attributed either to variations in the spallation rate or to some stellar property

(e.g. initial rotation rate or magnetic field) that affects the physical processes responsible for variations of the surface lithium abundances.

These questions are of prime importance when it comes to determining the primordial lithium abundance, and they recently became even more crucial in view of the results of the *Wilkinson Microwave Anisotropy Probe* (WMAP; Bennett et al. 2003; Spergel et al. 2003) on Cosmic Microwave Background (CMB) anisotropies. Indeed the CMB-based determination of the baryon-to-photon ratio, η , corresponds to a BBN-predicted primordial lithium abundance much larger (by a factor ~ 2.7 to 3.5) than the lithium abundances observed in the most metal-poor halo stars (Cyburt et al. 2003; Cuoco et al. 2003; Romano et al. 2003; see Charbonnel & Primas 2004 for more details). As we shall discuss below in detail, this is crucial for stellar physics as it gives strong constraints on the physical mechanism(s) responsible for surface lithium depletion in these objects.

2. Current status of Pop II stellar models

When the first models of Pop II dwarf stars including atomic diffusion were computed (Michaud et al. 1984), it became clear that slow mixing processes are acting in the radiative zones of these stars. Indeed, under conditions applicable for halo stars, pure atomic diffusion causes He, Li and heavier elements to

Send offprint requests to: C. Charbonnel,
e-mail: Corinne.Charbonnel@obs.unige.ch

¹ This denomination refers to the remarkably constant and flat lithium abundances among the metal-poor galactic halo dwarfs with effective temperature between ~ 5700 and 6300 K.

sink with respect to H. As the settling time-scale decreases with density, it is much shorter (at a given $[\text{Fe}/\text{H}]$) in the more massive stars of the plateau which have thinner convective envelopes. As a result, theoretical models including pure element segregation predict that the degree of surface Li depletion increases with T_{eff} . This result has been confirmed several times (Deliyannis et al. 1990; Proffitt & Michaud 1991; Chaboyer & Demarque 1994; Vauclair & Charbonnel 1995; Salaris & Weiss 2001); the case has been made even stronger recently with a generation of more sophisticated models for Pop II stars that include gravitational settling, thermal diffusion and radiative accelerations (Richard et al. 2002). The negative slope of Li with effective temperature obtained in these models is in contradiction with the Li data and calls for some macroscopic process that moderates atomic diffusion. Consistently, such a process is also required to counteract the settling of heavier elements in order to explain the close similarity of iron abundances in near turn off, sub-giant and lower RGB stars in globular clusters, and to reproduce the observed morphologies of globular cluster color–magnitude diagrams (see VandenBerg et al. 2002).

This is the recognition that models for Pop II stars should be no less sophisticated than current solar models which are strongly constrained by helioseismology. Those indeed require both atomic diffusion and slow mixing in the radiative zone to fulfill modern observational constraints (e.g., Christensen-Dalsgaard et al. 1993; Bahcall et al. 1995; Richard et al. 1996; Basu 1997; Brun et al. 1999).

Salaris & Weiss (2001) proposed an alternative solution to reconcile the pure (i.e., uninhibited) atomic diffusion models with the halo data. They showed that there is no apparent contradiction between theoretical lithium predictions and observations, provided that the most metal-poor field stars are more than 13.5 Gyr old. In that case, the more massive stars which are theoretically responsible for the negative lithium trend on the hot side of the plateau would have reached the sub-giant branch; there, they dredge-up the lithium that has settled below their convective envelope during the main sequence lifetime, and their surface abundance is temporarily close to that of less massive stars still on the main sequence. For lower ages however the discrepancy discussed above of course remains. As the authors state, this is not proof that diffusion is fully efficient in halo stars. This means only that pure diffusion models cannot be definitively discarded in view of the lithium halo data alone. However the identical values of $[\text{Fe}/\text{H}]$ exhibited by turnoff and more evolved stars in globular clusters like NGC 6397 or 47Tuc disagree with this statement (Minniti et al. 1993; Castilho et al. 2000; Gratton et al. 2001; Thévenin et al. 2001; Carreta et al. 2004).

Among the physical processes that have been invoked to counteract atomic diffusion in stellar interiors, one of the most natural is rotation as already suggested in a more general context by Eddington (1929). Rotating models for Pop II stars, including or not atomic diffusion, have been computed by several groups using different prescriptions for the distribution of initial angular momenta, for the loss of angular momentum from a magnetic wind, and even more importantly for the evolution of the angular momentum distribution and the resulting chemical transport (Vauclair 1988; Chaboyer & Demarque 1994;

Pinsonneault et al. 1991, 1999, 2002; Charbonnel & Vauclair 1995; Théado & Vauclair 2001). Since we have no information on the history of the lithium abundances and of rotational velocities (see Sect. 6) of halo stars, these prescriptions are generally calibrated from observational constraints based on open cluster stars and on the Sun.

Classical rotating models predict that a range of initial angular momenta generates a range of lithium depletion and that the scatter increases with the average lithium depletion. For Pop II stars this leads to a predicted dispersion in lithium abundances along the plateau which is higher than observed (Chaboyer & Demarque 1994; Vauclair & Charbonnel 1995; Bonifacio & Molaro 1997; Ryan et al. 1999). Pinsonneault et al. (1999, 2002) argue that this difficulty can be alleviated when the distribution of initial angular momenta is inferred from stellar rotation data in young open clusters. Considering the fact that the majority of young stars have low and similar rotation rates, they obtain a lithium depletion for halo stars of 0.1–0.2 dex, this small value being a consequence of the observational constraint on the narrowness of the plateau. In view of the determination of η coming from WMAP, this theoretical depletion factor cannot reconcile the data with the BBN-predicted primordial lithium abundance.

Vauclair (1999) investigated the interaction between meridional circulation and helium settling in solid-body slowly rotating stars and suggested that a quasi-equilibrium state could be reached in which both processes would, on average, cancel each other. Because lithium diffuses at the same rate as helium, lithium settling would also be canceled by this process. Vauclair & Théado (2001) presented numerical computations based on these developments. For the case of slowly rotating halo stars they predict a lithium depletion slightly smaller than a factor of two with a dispersion of 0.1 dex in the middle part of the plateau (the dispersion becoming larger at the two extremes of the plateau in effective temperature). These results have been obtained under the hypothesis that the stars have always rotated slowly (constant rotation velocity along the stellar lifetime with low values between 2.5 and 7.5 km s⁻¹), and neglecting any rotational braking in the early stages of evolution. As the authors say, this assumption is impossible to check directly, but it is in conflict with the observed spin-down of open cluster stars. However there is no theoretical reason why Pop I and Pop II stars should behave so differently. In the case of an important angular momentum loss, Vauclair & Théado expect a larger lithium destruction before their self-regulating process could take place, resulting probably also in a larger final dispersion.

In summary, all current stellar models have difficulties reconciling a non-negligible depletion of lithium (as needed from WMAP) with both the flatness and the extremely small dispersion of the lithium abundance along the plateau even when very special assumptions are made. Current rotating models which include only hydrodynamical mechanisms like meridional circulation and turbulence for the transport of angular momentum all share the same default: when applied to Pop I stars, they predict a substantial internal differential rotation for the Sun which is not compatible with helioseismology data (Libbrecht & Morrow 1991; Chaboyer et al. 1995; Tomczyk et al. 1995;

Krishnamurthi et al. 1997; Matias & Zahn 1998). This provides evidence for angular momentum transport by a mechanism which has still been neglected.

3. Rotation-induced mixing and angular momentum transport in low-mass Pop I stars

The main uncertainty in modern rotating models rests in the lack of information on the internal differential rotation. In stellar interiors, the degree of rotational mixing depends on several factors, among which the evolution of the internal distribution of angular momentum is the most important. As discussed in more detail in Talon & Charbonnel (1998, 2003 – hereafter Paper I), the strongest constraints on the physics of angular momentum transport in low-mass stars are the helioseismic rotation profile and the shape of the so-called Li dip. These independent clues point towards a mechanism that transports angular momentum much more efficiently than meridional circulation and turbulence in cool main sequence stars which have extended convective envelopes. In view of the importance of the evaluation of the primordial lithium abundance, it is worth checking whether this process could be acting in Population II stars. This is one of the main goals of the present paper.

In Paper I we discussed the efficiency of angular momentum extraction by internal gravity waves in main sequence low-mass stars of Population I. We showed that these waves, which are able to shape the solar rotation profile (Talon et al. 2002) present a peculiar mass dependence. We found that the total momentum luminosity in waves rises with stellar mass, up to the quasi-disappearance of the stellar convective envelope around 6500 K (corresponding to a mass of $\sim 1.4 M_{\odot}$ for solar metallicity) where the momentum luminosity drastically drops (see Fig. 3). As a result, the net momentum extraction associated with internal gravity waves presents a mass dependence that explains the Li dip in terms of rotational mixing: on the hot side of the Li dip and in more massive stars, the transport of angular momentum and of chemicals by meridional circulation and shear instabilities explains the lithium pattern (as well as the abundance anomalies of He and CNO; see Talon & Charbonnel 1998; Charbonnel & Talon 1999; Palacios et al. 2003); these stars should present internal differential rotation. In lower mass stars, gravity waves dominate the transport of angular momentum, thereby reducing the magnitude of meridional circulation and shear and shaping the Li pattern on the cold side of the dip. We thus predicted that Pop I main sequence stars with initial masses lower than $\sim 1.4 M_{\odot}$ must be quasi-solid body rotators, as is the Sun. Including this effect in addition to the transport of angular momentum by meridional circulation and turbulence is absolutely necessary to modelize correctly the rotation-induced mixing for stars on the cool side of the Li dip (Charbonnel & Talon 2004).

In this paper we present the results of a similar study for Pop II stars. Again, we focus on the differential properties of internal gravity waves among main sequence stars of various masses. We also discuss the expected consequences for the rotation of horizontal branch stars. Complete models including

both the effects of rotation and of waves will be presented in a forthcoming paper.

4. Internal gravity waves in Pop II stars along the Li plateau

4.1. Input physics

We refer the reader to Paper I for details on internal waves physics and on the computational method, and we just summarize here the key points.

1. *Excitation mechanism.* To evaluate the wave spectrum produced by stellar convective envelopes, we consider the excitation associated with Reynolds stresses as described by Goldreich et al. (1994) (see Sect. 2.2, Paper I). Excitation by overshooting is neglected due to the lack of a reliable prescription. Note that we expect overshooting to produce mostly high- ℓ waves which are not efficient in momentum extraction from the deep interior. This point is discussed further in Paper I.
2. *Shear layer.* The wave-mean flow interaction leads to the formation of a thin, double peaked shear layer that oscillates on a short time-scale (of the order of years). This layer, whose amplitude is self regulated by shear turbulence (this point will be discussed in detail in Talon & Charbonnel 2004), acts as a filter of the low ℓ waves that carry angular momentum in the inner radiative zone (see Sect. 3, Paper I).
3. *Momentum extraction.* We follow the time evolution of the shear layer according to Eq. (7) of Paper I over several oscillation cycles. In the presence of differential rotation between the convection zone and the bottom of the shear layer, differential wave dissipation between low prograde and retrograde waves leads to a net momentum deposition below this layer which varies with differential rotation (see Sect. 4.1, Paper I). We calculate the net, average luminosity below the filtering shear layer (at $r = R_{\text{cz}} - 0.03 R_{\star}$) for a given value of the differential rotation. It corresponds to momentum extraction in the stellar interior when the core rotates faster than the surface.

We examine the properties of internal gravity waves in stars with masses between 0.6 and 0.9 M_{\odot} and with $[\text{Fe}/\text{H}] = -2$. We consider a value of 0.2431 for the initial He mass fraction and the relative concentrations of α -elements are increased relative to the solar mix as appropriate for Pop II stars. We use the same code and input physics (eos, opacities, nuclear reactions) as in Palacios et al. (2002). Table 1 summarizes the model characteristics that are relevant for our purpose.

4.2. Momentum extraction by internal gravity waves along the Li plateau

The generation of internal gravity waves depends on the structure of the stellar convective envelope. For the stars we consider here this region is relatively extended as can be seen in Fig. 1 (see also Table 1) where some of their characteristics are plotted as a function of effective temperature both on the zero age main sequence (zams; open squares) and at 10 Gyr (black

Table 1. Characteristics of the stellar models (with $[\text{Fe}/\text{H}] = -2$) on the ZAMS and at 10 Gyr: effective temperature, luminosity, thickness of the external convective zone in stellar mass and radius, largest convective scale ℓ_c , characteristic convective frequency ν_c , and thermal diffusivity below the convective envelope K_T . ν_{max} is the maximum frequency required to capture the wave – mean flow interaction.

M_* (M_\odot)	Age (Gyr)	T_{eff} (K)	L/L_\odot	$\log(M_{\text{cz}}/M_*)$	R_{cz}/R_*	ℓ_c	ν_c (μHz)	K_T ($\text{cm}^2 \text{s}^{-1}$)	ν_{max} (μHz)
0.60	zams	4985	0.14	-1.18	0.271	57	0.517	2.43×10^5	1.25
	10	5125	0.18	-1.30	0.263	59	0.614	4.38×10^5	1.25
0.65	zams	5245	0.21	-1.44	0.236	67	0.751	7.79×10^5	1.25
	10	5436	0.29	-1.66	0.229	69	0.879	1.71×10^6	1.25
0.70	zams	5490	0.30	-1.77	0.206	78	1.05	2.37×10^6	1.25
	10	5725	0.47	-2.22	0.181	90	1.68	1.14×10^7	1.25
0.75	zams	5720	0.42	-2.18	0.176	92	1.50	6.89×10^6	1.25
	10	6015	0.78	-3.15	0.125	132	4.27	1.68×10^8	1.85
0.80	zams	5935	0.57	-2.79	0.131	126	3.29	4.31×10^7	1.85
	10	6342	1.37	-4.15	0.065	259	26.1	1.42×10^{10}	6.25
0.82	zams	6010	0.64	-3.04	0.119	140	3.96	6.56×10^7	1.85
	10	6503	1.80	-5.96	0.041	392	8.02	2.91×10^{11}	17.5
0.85	zams	6140	0.76	-3.55	0.094	175	7.02	2.22×10^8	2.50
	10	6810	2.92	-8.23	0.010	1110	384	2.80×10^{13}	*
0.9	zams	6370	0.99	-4.56	0.062	270	20.9	2.39×10^9	3.75

* No oscillation occurs in this model.

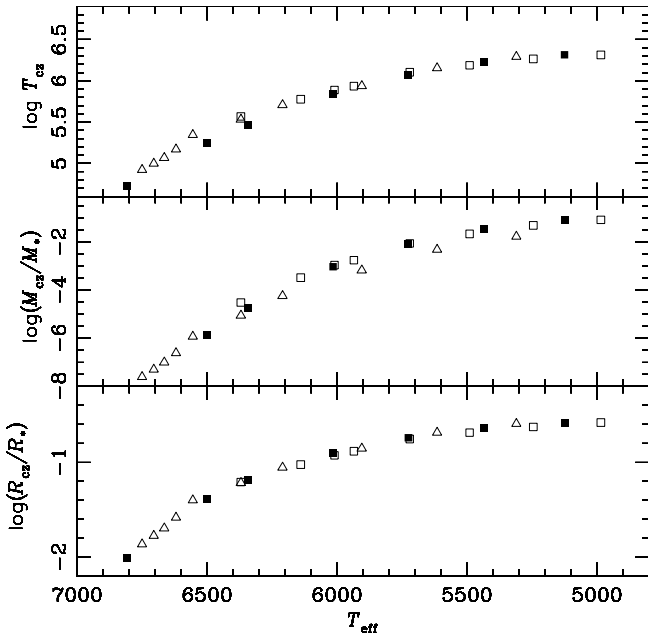


Fig. 1. (top) Temperature at the base of the convection zone (T_{cz}), (middle) mass of the convection zone and (bottom) radius of the convection zone as a function of T_{eff} . Squares: Pop II stars on the zams (open squares) and at 10 Gyr (black squares) (masses are those listed in Table 1); triangles: Pop I stars on the zams (models from Paper I).

squares). At a given age, the size of the convective envelope decreases when one goes to higher effective temperature. For a given stellar mass, as the star evolves the effective

temperature rises and thus the thickness of the convective envelope decreases.

Not all the stars for which we made the present computations will lie on the lithium plateau itself. If we consider an age of 10 Gyr, only the stars with masses between $\sim 0.7 M_\odot$ and $\sim 0.82 M_\odot$ (for $[\text{Fe}/\text{H}] = -2$) have an effective temperature in the plateau range (i.e., between ~ 5700 and 6500 K), while less massive stars exhibit lower lithium abundances and more massive ones have already evolved off the main sequence. In this limited mass range (which is indicated by the shaded area in Fig. 3 where we show the corresponding range in effective temperature on the zams), the thickness of the convective envelope varies only modestly: from $\sim 20\%$ to $\sim 12\%$ of the stellar radius for the zams models. In the same mass range and still on the zams, the characteristic convective frequency varies from $\nu_c \sim 1.6 \mu\text{Hz}$ to $\sim 12 \mu\text{Hz}$ while the spherical harmonic number ℓ_c corresponding to the largest convective scale varies from ~ 80 to ~ 140 .

To investigate how the wave spectrum produced by these convection zones varies as a function of stellar mass, let us first discuss wave characteristics based on the stellar models on the zero age main sequence. The corresponding momentum spectra are shown in Fig. 2 where $\mathcal{L}_J = 4\pi r_{\text{cz}}^2 \mathcal{F}_J$ is the momentum luminosity, r_{cz} and \mathcal{F}_J being respectively the radius at the base of the convective envelope and the momentum flux. We see that the spectrum characteristics, which depend on the structure of the convection zone, evolve with stellar mass. In particular, low frequency waves disappear when the stellar mass increases due to a larger thermal diffusivity below the thinner convective envelope (see Fig. 3) that leads to stronger damping (Eq. (1)).

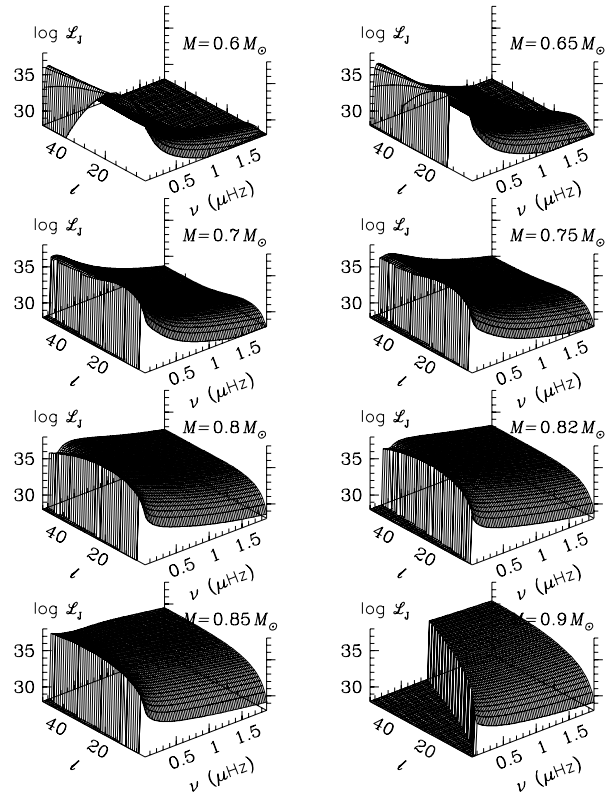


Fig. 2. Momentum wave spectrum in Pop II stars of various masses on the zams for the excitation model by Goldreich et al. (1994). The small radiative conductivity allows very low frequency waves to contribute to momentum transport.

In addition, the flux associated with a given frequency also rises with stellar mass together with the convective flux.

We then calculate the net momentum extraction associated with the waves for an initial differential rotation of $\delta\Omega = 0.01 \mu\text{Hz}$ over $0.05 R_*$ ². Figure 3 presents the corresponding net average luminosity at $0.03 R_*$ below the surface convection zone as a function of T_{eff} . We see that on the zams the net momentum luminosity modestly increases with the stellar mass (and thus with T_{eff}) up to $\sim 0.8 M_\odot$ and then slightly decreases for more massive stars before dropping dramatically in the $\sim 0.9 M_\odot$ star. For the limited mass range corresponding to the lithium plateau, the net momentum luminosity also presents a plateau.

During stellar life, the characteristics of the convective envelope evolve (see above), and consequently the net momentum luminosity changes with respect to its zams value. Of main importance are the changes of the thermal diffusivity below the convective envelope. At 10 Gyr, this quantity has indeed considerably increased for stars with masses higher than $0.8 M_\odot$ resulting in a strong decrease of the filtered momentum luminosity in these objects with respect to its zams value. However for the cooler stars which are less evolved at the same age, K_T remains closer to its initial value. Very importantly, the dependence of the net momentum luminosity as a function of

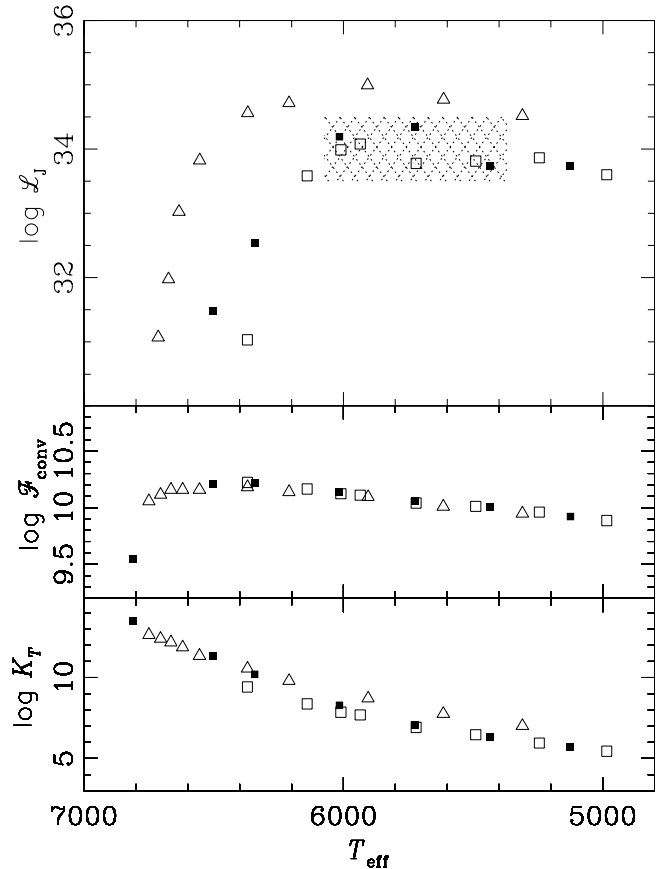


Fig. 3. (top) Net momentum luminosity at $0.03 R_*$ below the surface convection zone as a function of T_{eff} for an initial differential rotation of $\delta\Omega = 0.01 \mu\text{Hz}$ over $0.05 R_*$. (middle) Convective flux as a function of T_{eff} . (bottom) Thermal diffusivity as a function of T_{eff} . Symbols are defined in Fig. 1. The shaded area indicates the range in zams effective temperature of the Pop II stars which will lie on the lithium plateau at 10 Gyr.

effective temperature is very similar on the zams and at 10 Gyr: it presents a plateau as do the lithium abundances.

4.3. Comparison with Pop I stars on the cool side of the Li dip

Before comparing wave characteristics in Pop I and Pop II stars, let us underline some important points concerning the stellar models. At a given T_{eff} , Pop II stars along the Li plateau have lower masses than Pop I stars on the cool side of the Li dip. Regarding the depth of convective envelopes however, their lower metallicity tends to compensate for the mass effect. This can be seen in Fig. 1 where the thickness in both mass and radius of the convective envelope and the temperature at its base are plotted for both sets of models as a function of T_{eff} (triangles correspond to the Pop I zams models of Paper I). On the zams, these characteristics are extremely close for both stellar populations. As a result, the convective fluxes ($\mathcal{F}_{\text{conv}}$) are almost identical in both populations (Fig. 3). For a given effective temperature, the thermal diffusivity (K_T) below the convective envelope is always lower in Pop II stars than in their more metal-rich counterparts. Thermal diffusivity plays a major role

² This differential rotation is somewhat smaller than the value used in Paper I. In the figures, points corresponding to Pop I stars are calculated using the same model as those in Paper I, but with the new preferred value for the differential rotation.

in determining which frequencies contribute to momentum deposition in the interior. Indeed, the local wave amplitude is proportional to $\exp[-\tau(r, \sigma, \ell)]$ with

$$\tau(r, \sigma, \ell) = [\ell(\ell + 1)]^{\frac{3}{2}} \int_r^{r_c} (K_T + \nu_r) \frac{NN_T^2}{\sigma^4} \left(\frac{N^2}{N^2 - \sigma^2} \right)^{\frac{1}{2}} \frac{dr}{r^3} \quad (1)$$

where σ is the local, Doppler shifted frequency, $N^2 = N_T^2 + N_\mu^2$ is the Brunt-Väisälä frequency, N_T^2 is its thermal part and N_μ^2 is due to the mean molecular weight stratification (see Zahn et al. 1997 for details). Differential filtering occurs if the ratio K_T/σ^4 leads to significant differential damping between prograde and retrograde waves³, while a large thermal diffusivity totally inhibits low frequency waves. Thus the lower the thermal diffusivity, the lower are the low cut-off frequency (see Fig. 2) and the maximum frequency that leads to differential filtering (ν_{\max})⁴ (see Table 1).

Comparing the wave spectra to those obtained in Paper I, we find that the lower radiative conductivity in Pop II models allows waves of much lower frequency to contribute to momentum redistribution. In addition the lower thermal diffusivity below the convective envelope along the plateau mass range implies lower damping and the remaining of low frequency waves.

Of main importance for the differential effect of the waves from star to star is the increase of thermal diffusivity at higher T_{eff} . This translates into increasing radiative damping which becomes critical for T_{eff} higher than ~ 6200 K. The net momentum luminosity is shown for both populations in Fig. 3. Its general behavior as a function of effective temperature is very similar, while its magnitude is lower for Pop II stars. This is a consequence of the smaller radius of Pop II stars.

5. Consequences for the Li depletion in Pop II stars

5.1. From a coherent picture of mixing in Pop I stars ...

Combining the shape of the lithium dip and the dependence with stellar mass of the net wave momentum luminosity, we could conclude in Paper I that internal gravity waves are able to enforce solid-body rotation for Pop I stars with initial masses lower than $\sim 1.4 M_\odot$, i.e., with effective temperatures lower than ~ 6500 K. There, the differential rotation (that determines the extent of lithium destruction) will be the result of an equilibrium between momentum transport by meridional circulation, turbulence and internal gravity waves.

The time required for a star of a given mass to rotate as a solid body remains to be computed, but the solar case gives some clues. Helioseismology indeed constrains the complete rotation profile of a $1 M_\odot$ Pop I star, at 4.5 Gyr. This is however only an upper limit to the time-scale required to enforce solid body rotation in a solar-type star. Using the same physics as

³ This will be the case if differential rotation is of the same order as ω and K_T is large enough.

⁴ ν_{\max} , the maximum frequency required to capture the wave-mean flow interaction, is determined empirically.

we presently do, Talon et al. (2002) have shown that internal gravity waves can establish an almost uniform profile in a solar-like star in about 10^7 yr.

For the purpose of calculating lithium evolution, what is actually important is not the whole star, but rather the external region between the base of the convective envelope and the region of lithium destruction. Below the surface shear layer (i.e., just below the convective region), internal gravity waves will contribute to reduce differential rotation, thus limiting lithium destruction. Lithium abundances in open clusters give constraints on the time evolution of the rotation profile in these outer radiative regions. As can be seen from the lithium data in young clusters, this time-scale is extremely short for stars on the cold side of the lithium dip for which the net momentum luminosity reaches important values. In a very young cluster like the Pleiades (age ~ 0.135 Gyr according to the WEBDA, Mermilliod⁵), the lithium dip, though not very pronounced, begins to appear (i.e., King et al. 2000). This feature is very clear in Coma Ber (i.e., Ford et al. 2001), which is ~ 0.45 Gyr (WEBDA, Mermilliod). At this age, stars with effective temperatures higher than ~ 6500 K already show very strong lithium depletion, unlike their slightly cooler counterparts which have undergone only modest depletion despite their stronger braking. This gives an upper limit, which is highly conservative, to the time-scale for the internal gravity waves to balance the transport by meridional circulation and shear turbulence in the external parts of the radiative region; this time-scale should be used to constrain the wave generation model.

5.2. ... to a prescription for Pop II stars

To extrapolate this estimate to the case of Pop II stars, we have to introduce an important quantity: the ratio of the stellar luminosity to the stellar mass, which is shown in Fig. 5 for both Pop I and Pop II stars. The time-scale for meridional circulation and turbulence depends on L_*/M_* . This ratio strongly increases with the stellar mass leading to more efficient rotation-induced mixing in more massive stars. This statement has to be moderated here by the knowledge that stars with an extensive convective envelope are strongly spun down by magnetic torques when surface rotational velocities are large, as initially suggested by Schatzman (1962). The internal differential rotation induced by the braking of the external convective region enhances internal mixing, which will thus be strongly dependent on the existing processes for angular momentum transport.

More importantly here, L_*/M_* is much lower for the halo stars than for the metal-rich stars. This means that the characteristic time-scale for meridional circulation and turbulence will be longer (i.e., the associated mixing less efficient) in the halo stars. On the other hand, the net momentum luminosity is lower in these latter objects. How can both effect compensate?

Let us consider the case of two stars which lie in the region of full efficiency of the internal gravity waves, and which have similar effective temperature on the zams: the 1.20 and $0.82 M_\odot$ models. Their $L_*/M_*(\text{zams})$ values are respectively 1.34 and 0.78 , while their \mathcal{L}_J values are 9.8×10^{34}

⁵ <http://obswww.unige.ch/webda>

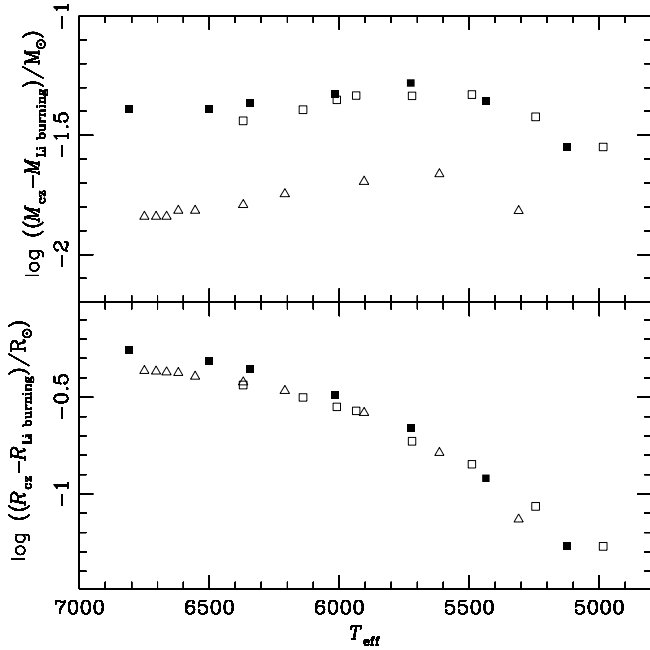


Fig. 4. Measure of the “distance” between the lithium burning region and the base of the convection zone with respect to T_{eff} . (*top*) In mass units. (*bottom*) In radius units. Symbols are defined in Fig. 1.

and $9.7 \times 10^{33} \text{ g cm}^2 \text{ s}^{-2}$. We can thus very crudely estimate that the time-scale for the gravity waves to dominate over the hydrodynamical processes in the region between the base of the convective envelope and that of lithium destruction in the metal-poor star will only be only a factor five longer than that necessary in the case of the metal-rich star. This gives an upper limit of the order of 2.2 Gyr if we consider the Coma Ber case. Let us note that this comparison is allowed by the fact that the distance between the base of the convective envelope and the region where Li burns is very similar for Pop I and Pop II stars at a given effective temperature (see Fig. 4). Again, this value is a very conservative upper limit.

It is important to insist on the fact that the net momentum luminosity associated with the internal gravity waves presents a plateau in the range in effective temperature corresponding to that of the lithium plateau (in Fig. 3, the shaded area indicates the effective temperature on the zams of the stars which will still lie on the lithium plateau at 10 Gyr). To explain the shape of the plateau, several features must be taken into account. Firstly, combining Figs. 3 and 5 shows that, for stars colder than 6100 K (the hot side of the plateau on the zams), wave momentum luminosity and L_*/M_* show the same trend, both rising very slowly with mass. This would lead to similar mixing efficiencies. Now adding Fig. 4, we see that, between 5400 and 6100 K (the location of the plateau on the zams), the “distance” between the base of the convection zone and the location of lithium burning is similar, while it starts shrinking in cooler stars. Roughly speaking, we thus expect similar lithium destruction on the plateau, becoming more efficient for cooler stars. Complete stellar models are required to check this conjecture, and will be presented in a forthcoming paper where the transport of both angular momentum and of the chemicals will

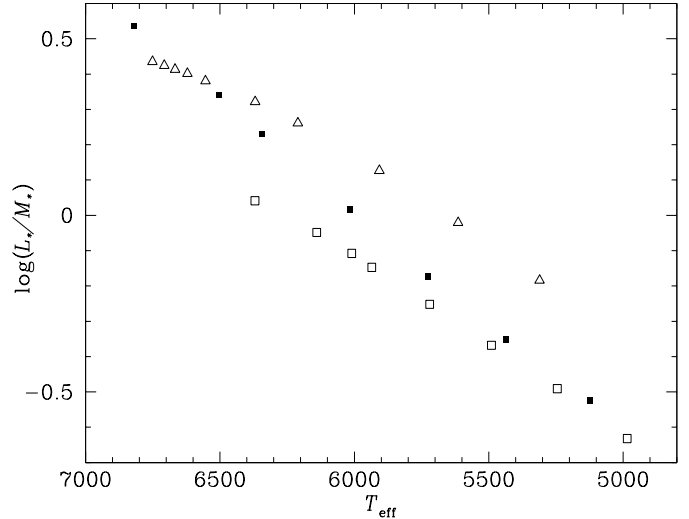


Fig. 5. Ratio of the stellar luminosity to the stellar mass as a function of effective temperature for Pop I and Pop II models. Symbols are defined in Fig. 1.

be computed under the effects of the meridional circulation, turbulence and gravity waves.

6. New perspectives on the rotation history of Pop II low-mass stars

6.1. Surface rotation velocity of Pop II main sequence stars

Very little data exist on the surface rotation velocity of metal-poor dwarfs. Rotation has been unambiguously detected only in tidally locked binaries (Peterson et al. 1980) or blue stragglers (Carney & Peterson 1981). For single main sequence turnoff stars, Peterson et al. (1983) obtained an upper limit on $v \sin i$ of 8 km s^{-1} for 30 main sequence halo stars with metallicity less than 1/10 solar. In their very high resolution and high signal-to-noise ratio studies of the lithium isotope ratios in metal-poor halo stars, Hobbs et al. (1999) found no evidence for extra-line broadening above 4 km s^{-1} , although line broadening at that level was needed to explain the data. Finally, Lucatello & Gratton (2003) derived upper limits to the rotation of turnoff and sub-giant stars in three globular clusters which are respectively of about 3.5 and 4.7 km s^{-1} . Of course, we have no information on the initial rotation of these stars. There is however no theoretical reason to believe that the distribution of initial momenta and the evolution of the surface rotation of low-mass Pop II stars have been very different from that of their Pop I counterparts.

6.2. Rotation of horizontal branch stars

Evolved stars can in principle provide some clues to the internal rotation of their progenitors. In the present context, information on the rotation of horizontal branch (HB) stars are very useful. Both field and globular cluster HB stars (both blue and red) can present substantial rotation rates, as discovered by Peterson et al. (1983) and Peterson (1983). For these objects $v \sin i$ does

not depend on any cluster parameter and neither the size nor the distribution of rotation is strongly correlated with the horizontal branch morphology, but the distribution of $v \sin i$ varies significantly from cluster to cluster (Peterson et al. 1995; Cohen & McCarthy 1997; Recio-Blanco et al. 2002; Behr 2003a). There is now some evidence that the hottest blue HB stars (which are supposed to have undergone the highest mass loss while on the red giant branch) rotate more slowly than their cooler counterparts (Behr et al. 2000; Recio-Blanco et al. 2002; Behr 2003a)⁶. Also, there is no apparent correlation between rotational velocity and luminosity distance from the zero age HB. Field HB stars behave similarly to such stars in globular clusters and the red ones appear to have about the same amount of surface angular momentum as do their blue counterparts (Preston 1997; Kinman et al. 2000; Carney et al. 2003; Behr 2003b).

In some rare cases, the observed rapid rotation rates are well explained either by tidal locking in a binary system (Carney et al. 2003) or by absorption of nearby planets (Soker 1998; Siess & Livio 1999). This is however not the case for most stars; indeed, several considerations argue against the possibility that all fast rotators gained the corresponding angular momentum through spin-up by a companion (Peterson et al. 1995).

6.3. Additional clues to the mass dependence of internal gravity waves efficiency

Another possibility is that the angular momentum was present at the time of stellar formation and remained hidden in the inner regions while only the surface was spun-down by the same process believed to operate in cool main-sequence Pop I stars; momentum then emerged at the end of the red giant branch when substantial mass loss occurred. Differential rotation with depth is a natural explanation for rapid rotation in HB stars to rotate rapidly while their main sequence progenitors were slow rotators. This requires substantial differential rotation with depth while on the main sequence to preserve a large enough reservoir of internal angular momentum (Pinsonneault et al. 1991; Sills & Pinsonneault 2000).

This latter interpretation has been discarded in light of the helioseismic determination of the internal solar rotation⁷. It can be however reconciled both with helioseismology and with our results for the following reason. Though the present mass of the globular cluster HB stars is lower than the inferred turnoff mass of the corresponding globular cluster, their initial mass was of

⁶ In all the globular clusters studied up to now, all the HB stars hotter than $T_{\text{eff}} \sim 11\,500$ K have $v \sin i \leq 8\text{--}12$ km s⁻¹ (Recio-Blanco et al. 2002). Among the cooler HB stars, there is a range of rotation rates and fast rotators appear.

⁷ In view of the solar data, Sills & Pinsonneault (2000) favor the class of models with constant specific angular momentum (i.e., differential rotation) in giant branch envelopes, retention of a rapidly rotating core on the RGB and subsequent angular momentum redistribution from the core to the envelope on the HB. Even this class of models requires relatively high surface rotation (~ 4 km s⁻¹) at the main sequence turnoff to explain the high rotation rates for the cooler HB stars.

course higher, implying a non negligible mass loss on the red giant branch ($\sim 25\%$ with a 1σ spread of about 10% around that mean; Rood 1973; Lee et al. 1990).

Typically, for the very metal-deficient globular cluster M 92 ([Fe/H] = -2.24 or -2.10 according respectively to Zinn & West (1984) and Carreta & Gratton (1997), a value which is close to the metallicity of the present models) the most recent age determinations vary between 12.3 Gyr for standard models (Salaris & Weiss 2002, hereafter SW02) and 13.5 Gyr for models including atomic diffusion and turbulent mixing (VandenBerg et al. 2002, hereafter V02). The corresponding turnoff mass and effective temperature are $\sim 0.78 M_{\odot}$ and 6650 K in the SW02 models (Salaris & Weiss, private communication) and $\sim 0.77 M_{\odot}$ and 6450 K in the V02 models (Richard, private communication). Because of some differences in the input physics (in particular, SW02 and V02 assume a lower cosmological helium mass fraction than we do, and V02 models include atomic diffusion), these masses cannot be directly compared with the ones of our models. What matters however is the effective temperature of these stars while they were on the main sequence, and which is strongly connected to the properties of the convective envelope that determine the gravity waves efficiency. In both sets of models, it is higher than the critical value where internal gravity waves are found to fail to enforce rigid rotation. According to the SW02 models, the turnoff effective temperature of the other globular clusters for which HB rotation velocities are now available (i.e., M 3, M 13, M 15, M 68, M 92 and NGC 288, Behr 2003a) is also always higher than this critical value.

This means that the stars which are at present on the HB in all the currently investigated globular clusters had such main sequence masses and effective temperatures, and thus such convective envelopes, that internal gravity waves were inefficient to extract angular momentum while on the main sequence. Like in the more massive and more metal-rich stars which lie on the left side of the lithium dip in open clusters, only hydrodynamical processes must have been acting in their main sequence progenitors. As a consequence the progenitors of the present HB stars must have left the main sequence with important internal differential rotation, contrary to what we predict for the stars along the lithium plateau, for the Sun and for the Pop I stars lying on the cool side of the lithium dip.

7. A final remark on HB stars and transport of angular momentum

While our main sequence predictions open new perspectives to explain the data on HB rotation, one has to remain cautious before definitively concluding on this point. It is necessary to investigate the possible effect of internal gravity waves while the star evolves on the red giant branch and on the HB, and to make complete simulations of the internal evolution of angular momentum all along the stellar life taking into account all the possible mechanisms together with a good description of the mass loss on the red giant branch. A self-consistent model should also explain why only a third of HB stars are fast rotators, and how fast rotation is coupled with cool effective

temperature on the HB. Work is in progress in this direction and will be presented in a forthcoming paper.

Let us make a final remark on the importance of HB stars rotation rates. Up to now, two processes have been proposed to explain the helioseismic solar rotation profile:

- 1) In the gravity wave model (Talon et al. 2002), there is a range of masses for which waves are efficient enough to lead to quasi-solid body rotation. In that framework, the lithium gap is explained by the combined effect of braking (which leads to increased differential rotation and rotational mixing) and the appearance of waves as the surface convection zone deepens for smaller masses (Paper I). For main sequence stars with only shallow surface convection zones, no waves are generated and large internal differential rotation is expected (see e.g. Talon et al. 1997; Meynet & Maeder 2000; Palacios et al. 2003), naturally explaining the fast rotation of HB stars.
- 2) In the magnetic model (Charbonneau & MacGregor 1993), there is no relation between the presence of a surface convection zone and solid body rotation as the dipolar field of the radiative zone has to be of fossil origin. In that case, the lithium gap might be explained in purely solid body rotation by the combined action of radiative forces and solid body meridional circulation (Charbonneau & Michaud 1988). However, one would then expect all the HB stars, originating from main sequence stars in solid body rotation, to rotate more slowly than observed.

All these results over a large range of the HR diagram strongly favor the gravity wave model. This does not mean of course that magnetic fields do not play a role in the whole picture. It seems to us however that we have sufficient clues to justify complete tests of a fully hydrodynamical model before including MHD effects.

8. Conclusion

In this paper, we discuss the generation and filtering of internal gravity waves in Pop II dwarf stars and its consequences on the angular momentum distribution both on the main sequence and on the horizontal branch. By comparing them with Pop I stars, we expect gravity waves to be efficient in producing quasi solid-body rotation in stars of the lithium plateau on very short time-scales. Consequently, a new generation of stellar models must take into account the effects of atomic diffusion, meridional circulation, turbulence and gravity waves, in order to estimate the theoretical depletion of lithium along the plateau.

On the other hand, we found the same dependence of gravity wave efficiency with effective temperature as in Pop I stars. In particular, gravity waves appear to be inefficient in the main sequence progenitors of present HB stars allowing strong differential rotation leading to a natural explanation of the fast HB rotators.

In this paper, we mainly focused on estimating whether gravity waves can play a significant role in shaping the internal rotation profile of lithium plateau and horizontal branch stars and did not intend to cover the complete problem which is far

more complex. Indeed, gravity waves can also lead to significant mixing by themselves (see e.g. Press 1981; Schatzman 1993; García López & Spruit 1991; Montalbán 1994) and proper treatment of these effects must be taken into account when building complete stellar models with waves. This will be discussed at length in a forthcoming paper.

We further note that the conjectures presented in this paper neglect the possible presence of a magnetic field. Indeed, our goal here is to verify whether a purely hydrodynamical mechanism can be responsible for the evolution of stellar parameters such as surface velocities and abundances and to produce definite diagnoses to test our models. Both theoretical and observational evidence shows that this is certainly the case.

Acknowledgements. We acknowledge financial support from the French Programme National de Physique Stellaire (PNPS). We thank the Réseau québécois de calcul de haute performance (RQCHP) and the Centre informatique national de l'enseignement supérieur (CINES) for useful computational resources. Thanks also to M. Salaris, A. Weiss and O. Richard for providing information on their stellar models.

References

- Bahcall, J. N., Pinsonneault, M. H., & Wasserburg, G. J. 1995, *Rev. Mod. Phys.*, 67, 781
- Basu, S. 1997, *MNRAS*, 288, 572
- Behr, B. B. 2003a, *ApJS*, 149, 67
- Behr, B. B. 2003b, *ApJS*, 149, 101
- Behr, B. B., Djorgovski, S. G., Cohen, J. G., et al. 2000, *ApJ*, 528, 849
- Bennett, C. L., Bay, M., Halpern, M., et al. 2003, *ApJ*, 583, 1
- Bonifacio, P., & Molaro, P. 1997, *MNRAS*, 285, 847
- Brun, A. S., Turck-Chièze, S., & Zahn, J. P. 1999, *A&A*, 525, 1032
- Carney, B. W., Latham, D. W., Stefanik, R. P., Laird, J. B., & Morse, J. A. 2003, *ApJ*, 125, 293
- Carney, B. W., & Peterson, R. C. 1981, *ApJ*, 251, 190
- Carreta, E., & Gratton, R. G. 1997, *A&AS*, 121, 95
- Carreta, E., Gratton, R. G., Bragaglia, A., Bonifacio, P., & Pasquini, L. 2004, *A&A*, 416, 925
- Castilho, B. V., Pasquini, L., Allen, D. M., Barbuy, B., & Molaro, P. 2000, *A&A*, 361, 92
- Chaboyer, B., & Demarque, P. 1994, *ApJ*, 433, 510
- Chaboyer, B., Demarque, P., & Pinsonneault, M. H. 1995, *ApJ*, 441, 865
- Charbonneau, P., & MacGregor, K. B. 1993, *ApJ*, 417, 762
- Charbonneau, P., & Michaud, G. 1988, *ApJ*, 334, 746
- Charbonnel, C., & Primas, F. 2004, in preparation
- Charbonnel, C., & Talon, S. 1999, *A&A*, 351, 635
- Charbonnel, C., & Talon, S. 2004, in preparation
- Charbonnel, C., & Vauclair, S. 1995, *A&A*, 295, 715
- Christensen-Dalsgaard, J., Proffitt, C. R., & Thompson, M. J. 1993, *ApJ*, 403, L75
- Cohen, J. G., & McCarthy, J. K. 1997, *AJ*, 113, 1353
- Cuoco, A., Iocco, F., Mangano, G., et al. 2003
[arXiv:astro-ph/0307213]
- Cybur, R. H., Fields, B. D., & Olive, K. A. 2003
[arXiv:astro-ph/0302431]
- Deliyannis, C. P., Demarque, P., & Kawaler, S. D. 1990, *ApJS*, 73, 21
- Eddington, A. S. 1929, *MNRAS*, 90, 54
- Ford, A., Jeffries, R. D., James, D. J., & Barnes, J. R. 2001, *A&A*, 369, 871
- García López, R. J., & Spruit, H. C. 1991, *ApJ*, 377, 268

- Goldreich, P., Murray, N., & Kumar, P. 1994, *ApJ*, 424, 466
- Gratton, R. G., Bonifacio, P., Bragaglia, A., et al. 2001, *A&A*, 369, 87
- Hobbs, L. M., Thorburn, J. A., & Rebull, L. M. 1999, *ApJ*, 523, 797
- King, J. R., Krishnamurthi, A., & Pinsonneault, M. H. 2000, *ApJ*, 119, 859
- Kinman, T., Castelli, F., Cacciari, C., et al. 2000, *A&A*, 364, 102
- Krishnamurthi, A., Pinsonneault, M. H., Barnes, S., & Sofia, S. 1997, *ApJ*, 480, 303
- Lee, Y. W., Demarque, P., & Zinn, R. 1990, *ApJ*, 350, 155
- Libbrecht, K. G., & Morrow, C. A. 1991, in *Solar interior and the atmosphere* (Univ. of Arizona Press), 479
- Lucatello, S., & Gratton, R. G. 2003, *A&A*, 406, 691
- Matias, J., & Zahn, J.-P. 1998, in *Sounding solar and stellar interiors*, poster volume, ed. J. Provost, & F. X. Schmider, *IAU Symp.*, 181
- Meynet, G., & Maeder, A. 2000, *A&A*, 361, 101
- Michaud, G., Fontaine, G., & Beaudet, G. 1984, *ApJ*, 282, 206
- Minniti, D., Geisler, D., Peterson, R. C., & Claria, J. J. 1993, *ApJ*, 413, 548
- Montalbán, J. 1994, *A&A*, 281, 421
- Palacios, A., Talon, S., Charbonnel, C., & Forestini, M. 2003, *A&A*, 399, 603
- Peterson, R. C. 1983, *ApJ*, 275, 737
- Peterson, R. C., Rood, R. T., & Crocker, D. A. 1995, *ApJ*, 453, 214
- Peterson, R. C., Tarbell, T. D., & Carney, B. W. 1983, *ApJ*, 265, 972
- Peterson, R. C., Willmarth, D. W., Tarbell, T. D., Carney, B. W., & Chaffee, F. H. 1980, *ApJ*, 239, 928
- Pinsonneault, M. H., Deliyannis, C. P., & Demarque, P. 1991, *ApJ*, 367, 239
- Pinsonneault, M. H., Walker, T. P., Steigman, G., & Narayanan, V. K. 1999, *ApJ*, 527, 180
- Pinsonneault, M. H., Steigman, G., Walker, T. P., & Narayanan, V. K. 2002, *ApJ*, 574, 389
- Press, W. H. 1981, *ApJ*, 245, 286
- Preston, G. W. 1997, *AJ*, 113, 1860
- Primas, F., & Charbonnel, C. 2004, *A&A*, in preparation
- Proffitt, C. R., & Michaud, G. 1991, *ApJ*, 371, 584
- Recio-Blanco, A., Piotto, G., Aparicio, A., & Renzini, A. 2002, *ApJ*, 572, L71
- Richard, O., Vauclair, S., Charbonnel, C., & Dziembowski, W. A. 1996, *A&A*, 312, 1000
- Richard, O., Michaud, G., Richer, J., et al. 2002, *ApJ*, 568, 979
- Rood, R. T. 1973, *ApJ*, 184, 815
- Romano, D., Tosi, M., Matteucci, F., & Chiappini, C. 2003, *MNRAS*, 346, 295
- Ryan, S., Norris, J. E., & Beers, T. C. 1999, *ApJ*, 523, 654
- Salaris, M., & Weiss, A. 2001, *A&A*, 376, 955
- Salaris, M., & Weiss, A. 2002, *A&A*, 388, 492, SW02
- Schatzman, E. 1962, *AnAp*, 25, 18
- Schatzman, E. 1993, *A&A*, 279, 431
- Siess, L., & Livio, M. 1999, *MNRAS*, 308, 1133
- Sills, A., & Pinsonneault, M. H. 2000, *ApJ*, 540, 489
- Sockett, N. 1998, *AJ*, 116, 1308
- Spergel, D. N., Verde, L., Peiris, H. V., et al. 2003, *ApJS*, 148, 175
- Spite, F., & Spite, M. 1982
- Talon, S., & Charbonnel, C. 1998, *A&A*, 335, 959
- Talon, S., & Charbonnel, C. 2003, *A&A*, 405, 1025 (Paper I)
- Talon, S., Kumar, P., & Zahn, J.-P. 2002, *ApJ*, 574, L175
- Talon, S., Zahn, J. P., Maeder, A., & Meynet, G. 1997, *A&A*, 322, 209
- Théado, S., & Vauclair, S. 2001, *A&A*, 375, 70
- Thévenin, F., Charbonnel, C., de Freitas Pacheco, J. A., et al. 2001, *A&A*, 373, 905
- Tomczyk, S., Schou, J., & Thompson, M. J. 1995, *ApJ*, 448, L57
- VandenBerg, D. A., Richard, O., Michaud, G., & Richer, J. 2002, *ApJ*, 571, 487, V02
- Vauclair, S. 1988, *ApJ*, 335, 971
- Vauclair, S. 1999, *A&A*, 351, 973
- Vauclair, S., & Charbonnel, C. 1995, *A&A*, 295, 715
- Zahn, J.-P., Talon, S., & Matias, J. 1997, *A&A*, 322, 320
- Zinn, R., & West, M. J. 1984, *ApJS*, 55, 45